ELSEVIER

Polymer 41 (2000) 5777–5785

polymer

Water absorption characteristics of diglycidylether of butane diol–3,5-diethyl-2,4-diaminotoluene networks

A. Tcharkhtchi*, P.Y. Bronnec, J. Verdu

ENSAM 151 bd de l'Hôpital 75013 Paris, France

Received 15 June 1999; received in revised form 30 September 1999; accepted 20 October 1999

Abstract

The water absorption characteristics of various networks based on diglycidylether of butane diol (DGEBD) and 3,5-diethyl-2,4-diaminotoluene with amine/epoxide functional ratio ranging from 0.7 to 1.3 and T_g values ranging from 36 to 91°C were studied in the 20–100°C temperature range. The equilibrium concentrations of water are of the order of 6–7% by weight with slight tendency to decrease with temperature, which can be attributed to the relatively high (negative) value of the heat of dissolution ($H_S \approx -46 \pm 1$ kJ mol^{-1}). Plasticization effects can be predicted from a simplified version of the free volume theory showing that the T_g depletion is an increasing function of the initial T_g value. There is no significant discontinuity at T_g of the temperature variations of the solubility and diffusivity, showing that the behaviour is controlled by the presence of strong hydrogen bonds between water molecules and the polar groups (essentially hydroxyls) of the polymer. The comparison of various epoxide–amine networks shows that the molar contribution of a given hydroxyl group is an increasing function of the hydroxyl concentration, which suggests that close hydroxyls could play a concerted role in water absorption.

For the samples having an epoxide excess, the gravimetric curves of water absorption display two steps, the first one being due to the physical sorption and the second one to the epoxide hydrolysis. The main characteristic features of this latter process are analysed. In the conditions under study (temperature, sample thickness), it is not diffusion controlled.

Keywords: Epoxy; Water absorption; Plasticization

1. Introduction

There is a relatively large amount of literature on water absorption mechanisms and kinetics in epoxy networks, owing to their obvious technical interest in high performance composites [1,2]. Despite this, many important aspects of these phenomena remain unclear. Concerning for instance the water equilibrium concentration, generally expressed in terms of mass percents W_∞, it has been hypothesized that it could be linked to the available "free volume" fraction, the latter being defined as it is usual in polymer physics [3] or linked to hypothetical packing defects [4,5]. An interesting characteristic of this so called "free volume" fraction is that it could be an increasing function of the crosslink density [6].

Despite the fact that they agree with an intuitive vision of water absorption mechanisms, the "volumetric approaches" of this phenomenon are highly questionable. As a matter of fact, it is easy to find free volume rich polymers, for instance silicone elastomers or crosslinked polyethylene, having a very low hydrophilicity. We have thus to consider that, as postulated by the theory of polymer–solvent miscibility, water absorption is linked to the existence of interactions between water molecules and polar groups present in the polymer. Let us recall that water is highly cohesive (Hildebrand solubility parameters of 40–45 MPa$^{1/2}$) and is characterized by especially low dispersive component and an especially high bonding component [7]. Structure–property relationships in this field allow to predict that H_2O molecules must interact essentially with highly polar groups as for instance hydroxyls in amine crosslinked epoxies [8,9]. Certain authors have suggested that crosslinking could be a direct cause of hydrophilicity in these networks [3], however it is noteworthy that in the structure series under investigation, the crosslink density is almost proportional to the alcohol concentration which can be a source of confusion.

According to Barrie [10] and Van Krevelen [11], water equilibrium concentration appears as a molar additive function and good predictions can be obtained from this rule if one considers elemental structural units sufficiently large to take into account eventual intramolecular interactions between hydroxyls and the neighbouring polar groups [8,9].

These relationships are however fully empirical and

* Corresponding author.

0032-3861/00/$ - see front matter
PII: S0032-3861(99)00801-0

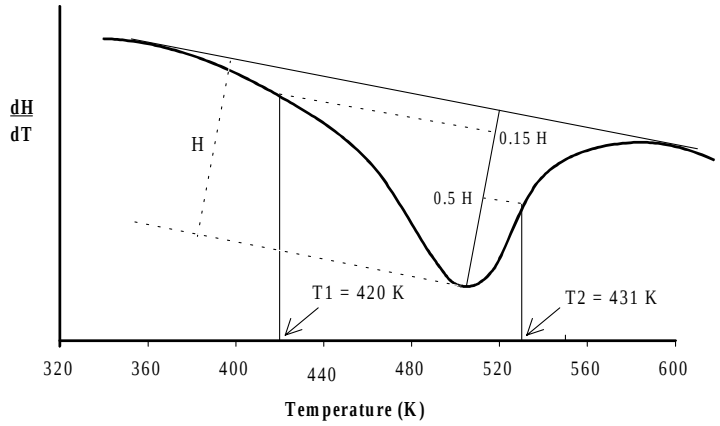

Fig. 1. Determination of cure temperatures from a DSC thermogram for the stoichiometric sample.

cannot be considered as a good basis for the understanding of the sorption mechanism. For instance, the fact that, for many groups, the number of water molecules absorbed per group is not an integer, is very difficult to explain in the frame of such a theory.

The application of the theory of solubility parameters seems to be a priori, a sounder approach but here also strong difficulties are encountered: firstly, the "solubility spectra" of epoxy networks are complex [12] and need a prohibitive amount of experimental work to be accurately established. In such situations, e.g. typically when polymer–solvent interactions are not predominantly of the dispersive type, the basic approach with a single (Hildebrand) solubility parameter displays bad predictive properties. The approach of partial (Hansen [13]) solubility parameters must be preferred. One can suspect that in epoxies, the hydrogen bonding partial solubility parameter δ_H plays an especially important role [12], however the accurate determination of these parameters is very difficult. Furthermore, it has been recently shown in the case of crosslinked PMMA, that even the partial solubility parameter approach is questionable, probably because it is also largely empirical [14]. Last but not least, the nature of the sorption equilibrium seems to have not clearly defined "physical meaning"—to our knowledge—in the case where the polymer–solvent mixture is in the glassy state this latter being by definition, out of thermodynamic equilibrium. In the rubbery state, in contrast, one knows that the sorption equilibrium results from the balance of osmotic forces resulting from the solvent penetration into the polymer and entropic forces resulting from chain drawing in the latter [15].

Concerning diffusion kinetics, there are numerous studies to establish the temperature effect on the diffusion rate or to model, especially using the Langmuir's theory, certain sorption anomalies [16], but the investigations on diffusion mechanisms and the structure–property relationships in this field are very scarce. Here, one can also distinguish between the "volumetric approaches" according to which water molecules would essentially migrate in morphological defects, for instance in the internodular phase [5,17], and "molecular approaches" according to which, for instance, water diffusion would be linked to segmental motion in the network [10].

The aim of the present work is to try to bring some answers to the above questions by a study of the sorption characteristics of a series of epoxide–amine samples differing only by the amine/epoxide molar ratio and chosen in order to have, in the temperature interval under study, certain samples in the glassy state and others in the rubbery state.

2. Experimental

2.1. Materials

The networks were based on the diglycidyl ether of butane diol (DGEBD) and 3,5-diethyl-2,4-diaminotoluene (ETHA) as the hardener. Their respective epoxide and amine index were equal to the theoretical values within experimental errors of titration and corresponded to the following formulae:

Diglycidyl ether of butane diol (DGEBD):

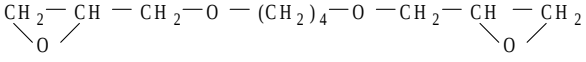

and 3,5-diethyl-2,4-diaminotoluene (ETHA):

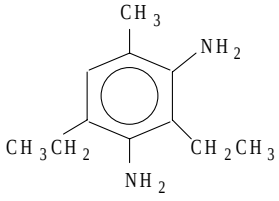

Networks were prepared from ETHA/DGEBD mixtures with amine/epoxide functional ratios.

$r = 0.7, 0.8, 0.9, 1.0, 1.1, 1.2$ and 1.3

This system displays a relatively low reactivity. From a

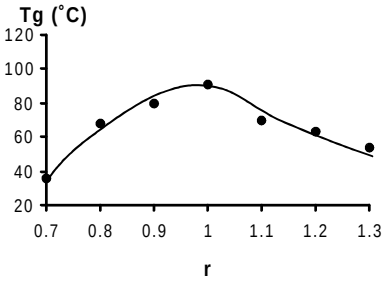

Fig. 2. Variation of the glass transition temperature with the amine/epoxide functional ratio.

DSC analysis of the reactive mixtures (see the example of the stoichiometric system in Fig. 1), it was decided to use for all the samples a two steps cure schedule, first step: 1 h at 142°C, second step: 2 h at 225°C.

The samples were thus prepared as follows:

- mixing for 30 min in an oil bath until a homogeneous mixture is obtained;
- degassing under primary vacuum (30 min at 145°C);
- moulding in metallic moulds with the above cure schedule.

The resulting samples have a brown skin due to oxidation, which is removed by machining. DSC thermograms of the sample core reveal the total disappearance of the crosslinking exotherm. No structural anomaly due to degradation or other side reactions was observed in FTIR spectra.

The glass transition temperature T_g varies with r, as expected in the case where side reactions, especially etherification or epoxide homopolymerization, are negligible: T_g is maximum at the stoichiometric point (Fig. 2)

The density in dry state varies almost linearly with r, from 1.168 ($r = 0.7$) to 1.154 ($r = 1.3$), which can be attributed to the variation of the number of "heavy" atoms (O and N) in the structure [18]. The average atomic mass M_a is defined by:

$$M_a = \frac{\text{molar mass of a representative structural unit}}{\text{number of atoms in this unit}}$$

varies with r in such a way as:

$$\frac{dM_a}{dr} = -\frac{1132}{(64+31r)^2} \approx -0.125 \text{ g mol}^{-1}$$

$$= -125 \times 10^{-6} \text{ kg mol}^{-1}$$

The variation of the density with r is given by:

$$\frac{d\rho}{dr} = -20 \text{ kg m}^{-3}$$

So that $d\rho/dM_a = 0.16 \times 10^6$ mol m^{-3}

To appreciate the average effect of atomic mass on density, one can consider the extreme values of polyethylene (PE) and polytetrafluoroethylene (PTFE) densities in amorphous state:

$$\left.\begin{array}{l}\rho(\text{PE}) \approx 850 \text{ kg m}^{-3} \\ \rho(\text{PTFE}) \approx 2350 \text{ kg m}^{-3}\end{array}\right\} \Rightarrow \Delta\rho = 1500 \text{ kg m}^{-3}$$

$$\left.\begin{array}{l}M_a(\text{PE}) \approx 4.667 \times 10^{-3} \text{ kg mol}^{-1} \\ M_a(\text{PTFE}) \approx 16.667 \times 10^{-3} \text{ kg mol}^{-1}\end{array}\right\} \Rightarrow \Delta M$$

$$= 12 \times 10^{-3} \text{ kg mol}^{-1}$$

So $\Delta\rho/\Delta M_a \approx 1.25 \times 10^5$ mol m^{-3}, a value in reasonable agreement with the value of 1.6×10^5 mol m^{-3} found for the series under study.

2.2. Samples and sorption tests

The samples were parallelepipeds of $30 \times 10 \times 2$ mm^3 dimensions, machined on both sides in order to obtain a good surface state, and displayed no visible defects (bubbles, cracks, etc.).

They were exposed in regulated ovens at 20, 30, 40, 50, 80 and 100 ± 1°C.

The exposure was made by immersion in distilled water, at reflux for the temperatures higher than 50°C.

2.3. Characterization

The samples were regularly removed from water, wiped and weighed with a METTLER H35AR laboratory balance.

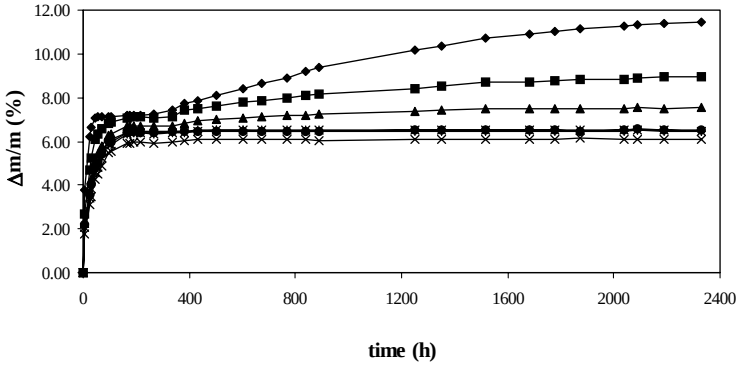

Fig. 3. Sorption curves for different systems at 50°C. $r = 0.7$ (◆), $r = 0.8$ (■), $r = 0.9$ (▲), $r = 1.0$ (×), $r = 1.1$ (●) and $r = 1.2$ (✳).

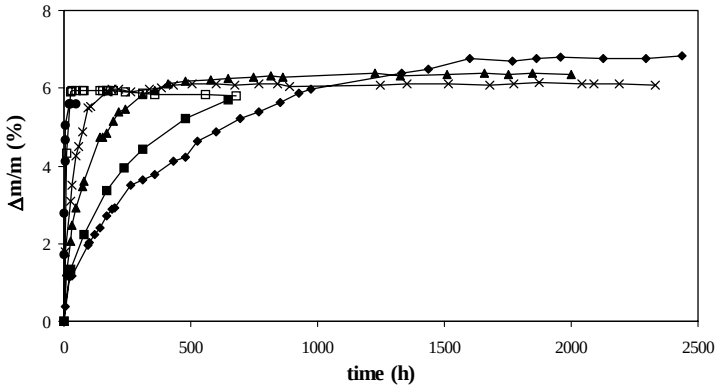

Fig. 4. Sorption curves at various temperatures for the stoichiometric samples 20°C (◆), 40°C (▲), 50°C (×), 80°C (□) and 100°C (●).

T_g in dry and wet state was determined by dynamic mechanical testing (DMTA) using a NETZCH apparatus at a frequency of 1 Hz. It was found that, in the conditions under study, water losses by evaporation are negligible. The density ρ in dry and wet state was determined by flotation in carbon tetrachoride–heptane mixtures.

3. Results and discussion

3.1. General features of water absorption

Examples of sorption curves are given in Fig. 3 (all samples under study at 50°C), and Fig. 4 (stoichiometric samples at various temperatures ranging from 20 to 100°C).

For the samples free of unreacted epoxides ($r > 1$), the process is single step and apparently Fickian. At the beginning of exposure, the mass gain m_t increases proportionally to the square root of exposure time. There is no apparent discontinuity linked to a change of physical state. For instance in the case of stoichiometric systems, T_g decreases from 91 to 45 ± 4°C. Despite this, no anomaly was observed in the sorption behaviour at the temperatures intermediate between 45 and 90°C.

The water equilibrium mass fraction m_∞ is, for all the samples, a slightly decreasing function of temperature. Here, also, there is no discontinuity in the curves $m_\infty = f(T)$, associated to the glass transition as well in the dry as in the wet state.

For the samples having an excess of epoxide groups ($r < 1$), we observe a two step's process, the first step being very similar to the one observed on systems free of unreacted epoxides. The second step, which is considerably slower than the first one, is obviously linked to these latter groups. The asymptotic mass gain determined for the second step has been compared, in Table 1, with the theoretical mass gain corresponding to the hydrolysis of the epoxide groups in excess. Both values are in reasonable agreement (taking into account the fact that a part of epoxide groups can be consumed in etherification reactions during cure) so that it can be assumed that the second step is due to epoxide hydrolysis.

Table 1
Experimental and theoretical values (see text) of the mass gain corresponding to the second step of the sorption process

	$r = 0.7$	$r = 0.8$	$r = 0.9$
Water absorption by the second step at 50°C (%)	4.2	1.8	0.8
Theoretical mass gain due to hydrolysis (%)	4.1	2.6	1.3

3.2. Density and glass transition temperature at equilibrium

The densities ρ and glass transition T_g in dry and wet states are given in Table 2.

The densities in wet state were reported only for the samples free of unreacted epoxides. They are slightly higher for wet than for dry samples. If one considers for instance the stoichiometric samples, the hypothesis of volume additivity would lead to:

$$\frac{1}{\rho} = \frac{m}{\rho_w} + \frac{1-m}{\rho_p}$$

where m is the water mass fraction, ρ_w and ρ_p the respective densities of water and polymer (in dry state) and ρ the polymer density in wet state. This relationship would lead to $\rho = 1.151$ against 1.168 experimental value. There are two ways to interpret this result: (i) water fills the "free volume" (ii) the water–polymer interaction favours the molecular packing.

The glass transition temperature decreases by 25–47 K upon water absorption. By combining the free volume approach of plasticization effect [19] with Simha–Boyer rule [20]: $(\alpha_l - \alpha_g)\, T_g = \text{constant}$, one obtains a simple relationship:

$$T_g^{-1} \approx T_{gp}^{-1} + A\varphi$$

where T_g and T_{gp} are the respective T_g values for the wet and dry polymer, φ is the water volume fraction (which can be assimilated in a first approximation to its mass fraction, i.e. $\varphi \approx m_\infty$. A is a coefficient representative of the plasticizing

Table 2
Equilibrium characteristics (density, glass transition temperature, plasticization parameters and solubility parameters) of the samples under study. Remarks: values obtained after exposure at 50°C

r	0.7	0.8	0.9	1.0	1.1	1.2	1.3
ρ (dry) (kg m^{-3})	1168	1166	1164	1162	1160	1158	1154
ρ (wet) (kg m^{-3})				1168	1164	1160	1158
T_g (dry) (°C)	36	68	80	91	70	63	54
T_g (wet) (°C)	11	26	43	44	37	27	26
m_∞	0.072			0.061			0.064
A (K^{-1})	3.95×10^{-3}			6.68×10^{-3}			4.47×10^{-3}
T_{gw} (K)	139			106			132
S (20°C) (mol m^{-3} Pa^{-1})	2.47			1.88			1.95
S (100°C) (mol m^{-3} Pa^{-1})	9.19×10^{-2}			7.91×10^{-2}			7.99×10^{-2}
S_0 (mol m^{-3} Pa^{-1})	9.4×10^{-9}			16.8×10^{-9}			15.2×10^{-9}
H_S (kg mol^{-1})	−47.2			−45.0			−45.5

effect of the penetrant (here water), in principle given by:

$$A = T_{gw}^{-1} - T_{gp}^{-1}$$

where T_{gw} is the glass transition temperature of water.

We have calculated A and T_{gw}, their values are given in Table 2

$$A = \frac{[T_g^{-1} - T_{gp}^{-1}]}{m_\infty}$$

$$T_{gw} = (A = T_{gp}^{-1})^{-1}$$

T_{gw} values of 100–150 K are obtained. They are in good agreement with physical data [21,22]. It seems thus that the plasticization effect of water on these networks is reasonably well described by a relationship derived from the free volume theory. Incidentally, the proposed model predicts that the plasticizing effect of water is an increasing function of T_{gp}, which is effectively observed here since the highest T_g depletion is observed for the highest T_{gp} value ($r = 1$).

Returning, now to the question of density increase upon water absorption one sees that the above results are consistent with the hypothesis that water is essentially dissolved into the network (no separated phase), which allows us to reject the hypothesis that water fills the "free volume".

3.3. Water solubility

The solubility coefficient S was determined from the following relationship:

$$S = \frac{10m_\infty}{18(1 + m_\infty)} \times \frac{\rho}{p} \qquad \text{(Henry's law)}$$

where p is the water pressure at the temperature under consideration. For the samples containing unreacted epoxides ($r < 1$), m_∞ was taken at the first plateau when it was distinguishable. Some typical values of S (at 20 and 100°C) are given in Table 2.

An Arrhenius plot of S is presented in Fig. 5. S obeys the Arrhenius law:

$S = S_0 \exp\left(-\frac{H_S}{RT}\right)$ H_S being the heat of solution.

The values of S_0 and H_S are given in Table 2 for $r = 0.7$; 1.0 and 1.3. H_S takes a high negative value, which explains the fact that m_∞ is a slightly decreasing function of the temperature. The observed trends are well consistent with the

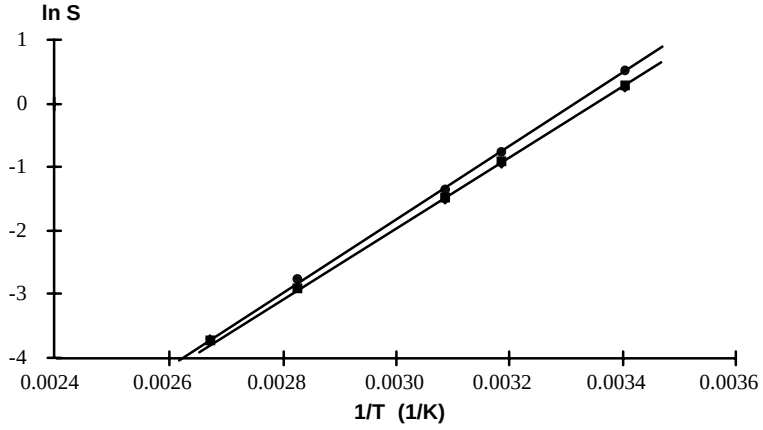

Fig. 5. Arrhenius plot of solubility coefficient.

Table 3
Hydroxyl concentration and water equilibrium concentration for various epoxy networks

Systems	[–OH] (mol kg^{-1})	[H_2O] (mol kg^{-1})	Ref.
DGEBD–ETHA	6.87	3.61	This work
DGEBA–ETHA	4.46	0.94	[24]
TGMDA–DDM	6.45	2.41	[8]
DGEBF–DDM	4.87	1.46	[8]
DGEBA (0.11)–DDM	4.49	1.17	[8]
DGEBA (2.3)–DDM	3.94	0.88	[8]
DGEBA (6.0)–DDM	3.73	0.74	[8]

available structure–property relationships in this field predicting that H_S must be negative for very cohesive solvents [11]. The water dissolution in the network is thus highly exothermic, which is due to the formation of strong hydrogen bonds between the water molecules and the polar groups of the networks, especially hydroxyls. S (and H_S) do not depend sharply on the network structure in the series under study despite relatively large variations of the cross-link density (about $x \approx 1.3$ mol kg^{-1} for $r = 0.7$ to $x \approx 3.4$ mol kg^{-1} for $r = 1$ and $x \approx 2.2$ mol kg^{-1} for $r = 1.3$, x being the concentration of trifunctional network nodes ($M_C = 2/3x$)). The fact that S is independent of the physical state is somewhat surprising. It could be expected that, in the rubbery state, the sorption equilibrium is determined by the balance between osmotic and entropic forces, as expressed by the Flory–Rehner equation [15]. But in fact there is no significant swelling and sorption is obviously governed by the polymer–water interactions, even above T_g.

It is interesting to remark that, in the system under study as in most of the epoxide–amine systems, the number of water molecules (at equilibrium) per hydroxyl group is smaller than unity, which indicates that certain hydroxyls do not act as hydrophilic sites. This result can be considered as a strong argument against predictive approaches based on the hypothesis of molar additivity of water absorption [10] despite their relatively good results in the field of epoxide–amine networks [8,9]. There is no doubt that the main hydrophilic site in these materials is the amino–alcohol group:

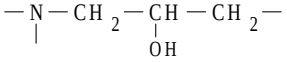

The contribution of this group to water absorption depends on its immediate neighbour (which determines especially the electron density on the nitrogen atom [3,8]). Thus, in a series of samples based on the same hardener and containing no other significantly hydrophilic group (such as for instance $-SO_2-$) than amino-alcohol, the hypothesis of molar additivity can be checked. The equilibrium water concentration is expected to be proportional to the hydroxyl concentration.

In the case of ETHA, we dispose only two series of data relative to the system under study (DGEBD–ETHA) and to parent systems in which DGEBD was replaced by the diglycidyl ether of bisphenol A (DGEBA) [23]. In the case of diaminodiphenylmethane (DDM) we dispose of more results [8,9]. All these data are summarized in Table 3. The equilibrium number of water moles per kg was plotted against hydroxyl concentration in Fig. 6. The dependence appears to be parabolic rather than linear. Thus the hypothesis of molar additivity of group contributions to water absorption is not rigorously valid, which is not surprising owing to the fact that molar contributions are not integers.

A possible explanation of the pseudo parabolic trend of Fig. 6 is based on the observation, for instance by NMR, that water is doubly bonded [24]. A pair of close hydroxyl groups could be, then, a favourable site for water absorption. It can be calculated that the average distance between two

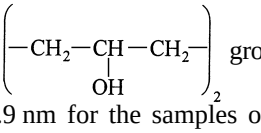

groups ranges between about 0.7 and 0.9 nm for the samples of Table 3. However their spatial distribution is not homogenous and there is a fraction of OH pairs sufficiently close to allow the formation of complexes with water molecules. The effect of the concentration of OH groups (e.g. of the average distance between OH groups) could be thus schematized by the following oversimplified model: the spatial distribution of distances between OH groups is supposed to be gaussian with an arbitrary chosen standard deviation, σ, of 2.5 nm. If one considers that only the OH pairs with a distance lower than 6.2 nm are active in H_2O sorption, then, the concentration of OH groups C_a would be: $C_a = pC$ where C is the whole OH concentration

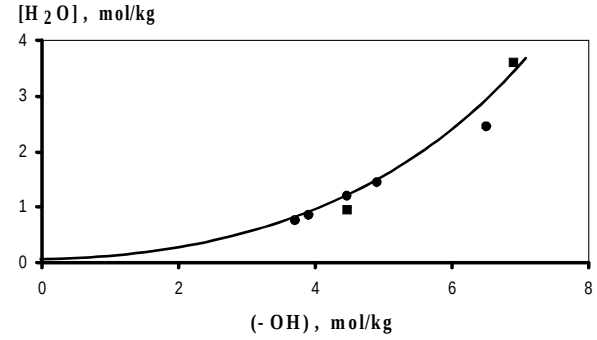

Fig. 6. Number of sorbed water moles per kg against hydroxyl concentration.

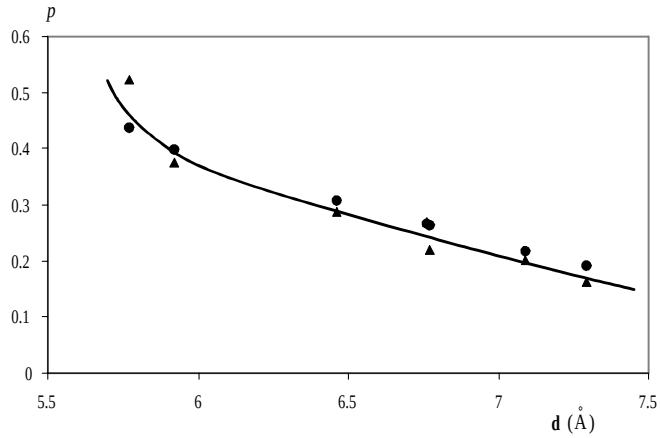

Fig. 7. Fraction of active OH groups. Determined from the water equilibrium concentration Ca (p = Ca/C) (●) and from a gaussian model for OH spatial distribution (▲).

and $p = \int_0^{6.2} 1/(\sigma\sqrt{2\pi}) \exp - ((d - \overline{d})^2)/(2\sigma^2)\, \mathrm{d}d$ where $\overline{d}$ is the average distance between neighbouring OH groups: $\overline{d} = (1/(N_a C\rho))^{1/3}$ where N_a is the Avogadro's number and r the density. p has been plotted against $\overline{d}$ and C in Fig. 7. As predicted, it varies pseudo parabolically with the OH concentration.

3.4. Water diffusivity

The uncorrected diffusion coefficient D_u was determined by the classical method derived from Fick's law:

$$D_u = \frac{\pi e^2}{16}\left(\frac{1}{W_\infty} \times \frac{\mathrm{d}W}{\mathrm{d}t}\right)^2$$

where e is the sample thickness.

Then the diffusion coefficient D was calculated using the shape factor of Shen and Springer [25]:

$$D = \frac{D_u}{\left(1 + \frac{e}{L} + \frac{e}{l}\right)^2}$$

where L and l are, respectively, the length and the width of the sample.

Some typical values of D are given in Table 4 and an Arrhenius plot of D is shown in Fig. 8. The apparent activation energy is of the order of 17 kJ mol^{-1}, however the curves display a slightly sigmoidal shape indicating some non-Arrhenian character. As in the case of solubility, no clear discontinuity can be observed at T_g (wet or dry). This is surprising since free volume is expected to play a key role in diffusion. A possible explanation of this behaviour is that the transport of water molecules into the matrix is kinetically governed by the polymer–water association–dissociation equilibrium, an elementary step of water transport being schematized as follows:

$$[W - P_1] \rightarrow W + P_1 \quad \text{(I)}$$

$$W \rightarrow \text{diffusion step from } P_1 \text{ to } P_2 \quad \text{(II)}$$

$$W + P_2 \rightarrow [W - P_2] \quad \text{(III)}$$

$$[W - P_2] \rightarrow W + P_2 \text{ etc.}$$

where W is the water molecule, P_1 and P_2 are neighbouring hydrophilic sites, and [W–P] is the hydrogen bonded polymer–water complex. One can imagine that, schematically, diffusion is not strongly influenced by the polymer molecular mobility if the dissociation of the polymer–water complex (I) is slower than the water diffusion (II).

3.5. Hydrolysis of epoxide groups

The hydrolysis process can be ascribed:

$$E + W \rightarrow Y$$

where E, W and Y represent respectively the epoxide group, the water molecule and the resulting diol.

As quoted in the first paragraph of this discussion, the experimental values of the mass gain at the second step

Table 4
Diffusion coefficients at 20, 50 and 100°C

	$r = 0.7$	$r = 0.8$	$r = 0.9$	$r = 1.0$	$r = 1.1$	$r = 1.2$	$r = 1.3$
$D \times 10^{12}$ (m^2 s^{-1}) at 40°C	2.72	–	–	0.69	–	–	0.81
$D \times 10^{12}$ (m^2 s^{-1}) at 50°C	2.72	2.89	2.18	179	1.87	1.97	2.11
$D \times 10^{12}$ (m^2 s^{-1}) at 80°C	17.1	–	–	10.5	–	–	10.4
$D \times 10^{12}$ (m^2 s^{-1}) at 100°C	–	–	–	26.9	29.9	30.5	31.7

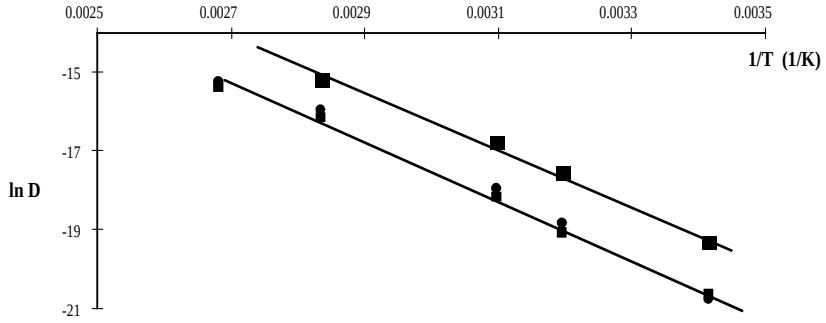

Fig. 8. Arrhenius plot of diffusion coefficient.

are in good agreement with the hypothesis of such a hydrolysis process.

In a first approach (neglecting the hydrophilicity of the formed diols), the following simplified kinetic model can be proposed:

$$\frac{dY}{dt} = kWE = kW(E_0 - Y)$$

Here $W = W_\infty$ (equilibrium water concentration), because the hydrolysis is not diffusion controlled (both sorption and hydrolysis processes are well separated in most of the gravimetric curves).

One can thus consider that $kW = K =$ constant; so that:

$$Y = E_0(1 - \exp(-Kt))$$

K can be estimated from the half life time $t_{1/2}$ such as for $t = t_{1/2}$, $Y = E_0/2$. Then:

$$K = \frac{\ln 2}{t_{1/2}}$$

The reciprocal of K: $\kappa = t_{1/2}/\ln 2$ can be considered as the time constant of the hydrolysis reaction. Its values are given in Table 5, where they can be compared to the diffusion time constant: $\tau_D = e^2/D$. One can see that:

(a) $\kappa \gg \tau_D$ which justifies our assumption that hydrolysis is not diffusion controlled;
(b) κ is practically independent of the residual epoxide concentration as expected in the frame of the chosen model.

4. Conclusions

We have studied the water absorption characteristics of some networks resulting in the condensation between diglycidyl ether of butane diol (DGEBD)–3,5-diethyl-2,4-diaminotoluene (ETHA). This system was chosen in order to study these characteristics on both sides of the glass transition temperature. The results can be summarized as follows:

- Water absorption occurs with a very small volume change but without clustering or microvoiding.
- Plasticization effects can be predicted from a simplified version of the free volume theory. This latter predicts that, as observed, the T_g depletion is an increasing function of the initial (dry) T_g value.
- The equilibrium water concentration is a slightly decreasing function of the temperature, which is explained by the highly exothermic character of the water dissolution in the polymer, due to the formation of relatively strong polymer–water hydrogen bonds. Water molecules could be linked to pairs of hydroxyl groups, which would explain the pseudo parabolic dependence of equilibrium water concentration with the hydroxyl concentration.
- There is no marked discontinuity at the glass transition temperature in the temperature dependence of solubility or diffusivity, which seems to indicate that the whole behaviour is governed by the strength of the polymer–water hydrogen bonds.

For the samples having an epoxide excess, the gravimetric curves display a second plateau linked to the epoxide hydrolysis into diols. It is interesting to note that in composites, the existence of a second plateau has been often interpreted in terms of Langmuir absorption mechanism. This interpretation is probably to be reconsidered in many cases since one knows that industrial composites are often

Table 5
Hydrolysis characteristic time and diffusion characteristic time

Temperature (°C)	$r = 0.7$		$r = 0.8$		$r = 0.9$	
	$\kappa \times 10^{-5}$ (s)	$\tau_D \times 10^{-5}$ (s)	$\kappa \times 10^{-5}$ (s)	$\tau_D \times 10^{-5}$ (s)	$\kappa \times 10^{-5}$ (s)	$\tau_D \times 10^{-5}$ (s)
40	56.3	2.9	–	–	–	–
50	45.4	1.5	35.7	1.4	30.7	1.8
80	5.4	0.05	–	–	–	–

undercured and contain, thus, epoxide groups. It is noteworthy, however, that from the kinetic viewpoint, hydrolysis and Langmuir models can give formally equivalent results.

References

[1] Adamson MJ. J Mater Sci 1980;15:1736.
[2] Enns JB, Gilham J-K. J Appl Polym Sci 1983;28:2831.
[3] Johncock P, Tudgey GT. Br Polym J 1986;18:242.
[4] Diamant Y, Marom G, Broutman LJ. J Appl Polym Sci 1981;26:3015.
[5] Gupta VB, Drzal LT, Rich MJ. J Appl Polym Sci 1985;30:4467.
[6] Pang KP, Gilham JK. J Appl Polym Sci 1989;37:1969.
[7] Barton AFM. Handbook of solubility and other cohesion parameters, Boca Raton, FL: CRC Press, 1985.
[8] Morel E, Bellenger V, Verdu J. Polymer 1985;26:1719.
[9] Bellenger V, Verdu J, Morel E. J Mater Sci 1989;24:63.
[10] Barrie JA. Water in polymers. In: Crank J, Park G-S, editors. Diffusion in polymers, London: Academic Press, 1968, chap. 8.
[11] van Krevelen DW. Properties of polymers. Their correlation with chemical structure. Their numerical estimation and prediction from additive group contributions, 3. Amsterdam: Elsevier, 1990.
[12] Bellenger V, Morel E, Verdu J. J Appl Polym Sci 1989;37:2563.
[13] Hansen C-M. J Paint Technol 1967;39:104, see also p. 511.
[14] Bellenger V, Kaltencker-Commercon J, Verdu J, Torjeman Ph. Polymer 1997;38(16):4175.
[15] Flory PJ, Rehner J. J Chem Phys 1943;11:521.
[16] Carter FG, Kibler KG. J Composite Mater 1978:12.
[17] Apicella A, Nicolais L. Adv Polym Sci 1985;72:70.
[18] Won VG, Galy J, Pascault J-P, Verdu J. Polymer 1991;32:79.
[19] Kelley FN, Bueche FJ. J Polym Sci 1961;50:549.
[20] Simha R, Boyer RF. J Chem Phys 1962;37:1003.
[21] Seki S. Bull Chem Soc Jpn 1968;41:2586.
[22] Angell CA, Donnella J. J Chem Phys 1977;57:4560.
[23] Salmon, L. Etude de la dégradation hydrolytique de l'interface fibre–matrice dans les composites fibres de verre-résine époxyde. Thesis ENSAM. Paris, October 1997.
[24] Fuller RT, Fornes RE. Memory. J Appl Polym Sci 1979;23:1871.
[25] Shen CH, Springer GS. J Composite Mater 1976;10:1.